Research Article

Ahmet Fevzi Savaş*, Hasan Öktem, Burak Öztürk, İlyas Uygur, Özkan Küçük

Energy consumption, mechanical and metallographic properties of cryogenically treated tool steels

https://doi.org/10.1515/chem-2022-0322
received March 7, 2023; accepted April 5, 2023

Abstract: This article examines energy consumption, microstructure, mechanical properties, and the change in the wear amount during the machining of GGG-42 cast iron material with two types of guide cutting tool produced by powder metallurgy and casting method The tap. tool samples used as cutting tool material were first subjected to the traditional hardening process and then to two different cryogenic treatments (24–16 h) at –90°C. The internal structures of the guide samples obtained from conventional heat treatment and cryogenic treatment were examined with an optical microscope and Scanning Electron Microscope. The hardness changes were checked with Vickers measurement method. The wear amount forming after the threading process was measured with CLEMEX program in a light microscope. In addition, by measuring the current amount drawn during the machining of the cast iron with guide cutter tools, instantaneous power consumption during cutting and power consumption during chip removal were calculated. The application of heat treatment and cryogenic process increased the hardness of the guides. Moreover, the power consumption during the chip removal was also seen to increase. This can be commented that cutting tools produced with powder metallurgy perform better than the cutting tools produced via casting and 30% energy saving.

Keywords: threading process, cryogenic process, microstructure, energy reduction, process development

*** Corresponding author: Ahmet Fevzi Savaş,** Department of Alternative Energy Sources Technologies, Bilecik Şeyh Edebali University, Vocational School, Bilecik, Turkey, e-mail: ahmetfevzi.savas@bilecik.edu.tr
Hasan Öktem: Department of Machine and Metal Technologies, Kocaeli University, Hereke Vocational School, Kocaeli, Turkey
Burak Öztürk, Özkan Küçük: Department of Metallurgical and Materials Engineering, Bilecik Şeyh Edebali University, Bilecik, Turkey
İlyas Uygur: Department of Mechanical Engineering, Faculty of Engineering, Düzce University, Düzce, Turkey

1 Introduction

Materials of high-speed tools used in the cutting process are required to have a certain toughness value. Besides, these tools are expected to be wear-resistant at high temperatures. DIN 1.3343 steel is a standard high-speed tool steel and has having versatile usage area with high toughness and cutting properties [1]. The development of high-speed steels began with the hardening of tungsten-manganese steel by Mushet in 1860. The machining possibilities of these steels were not fully known until Taylor and White used them in applications in 1900 [2].

In order to remove chips from a hard material, a cutting tool that is harder, has wear resistance, and produced at ideal cutting angles is required. These steels have quite high hardness values due to additions of high carbon and alloy elements. The special carbides formed by alloy elements with carbon increase the hardness. The hardness values of many tool steels can be increased up to 67–68 HRc [3]. The toughness in high-speed tool steels is increased by reducing the carbon amount in the composition of the steel to a lower level or by hardening the steel in an austenitizing temperature lower than the generally known austenitizing temperature, thereby providing a finer grain size [4]. One of the important properties of high-speed steels used as a cutting tool material is the cutting capability. According to the usage area of the tool, cutting capability is highlighted or shaped. Then, the tool is subjected to heat treatment in order to acquire properties like toughness, hardness, and wear resistance in accordance with the material of the workpiece. It provides an important effect on the formation of the desired martensite as a result of heat treatment. MC carbides, for example, vanadium carbide, increase the wear resistance of the steel due to their

extreme hardness [5]. In terms of their properties, these steels are similar to tungsten high-speed steels but they generally have slightly higher toughness at the same hardness. The main advantage of molybdenum steels is that they have almost 40% lower initial cost than tungsten steels of the same type. High carbon and vanadium amount increase wear resistance, and the increase in the amount of cobalt as in tungsten steels increases the red hardness. M15 is the most wear-resistant steel of the M group. M Steels are a bit more susceptible to hardening conditions than T steel, especially in heating and leaving to the atmosphere because they are easily decarburized under improper processing conditions. Almost 90% of all high-speed steels produced in the United States are molybdenum steel [6]. High alloying elements and carbon amount in speed steels reduce martensite start and completion temperatures. The martensite completion temperature drops below room temperature. Therefore, there is austenite remaining before transforming martensite in the structure while quenching from the austenitizing temperature to the steel. This is called "remaining austenite" or "residual austenite." Other than martensite and residual austenite, there are special carbides in the internal structure of the quenched steel that remain undissolved at austenitizing temperature and are formed by alloying elements. After hardening, there are 70% martensite, 10% undissolved carbide, and 20% residual austenite in the microstructure of the steel Bargel and Schulze, 1987 [7,8]. Cryogenic process is a cooling process used to improve wear resistance in tools exposed to high wear. The process is divided into two groups including shallow cryogenic and deep cryogenic processes. The shallow cryogenic process is more common, and this process is applied to the materials in the temperature range between –60°C and –90°C; however, the deep cryogenic process is applied at temperatures below –125°C. As shown in Figure 1,

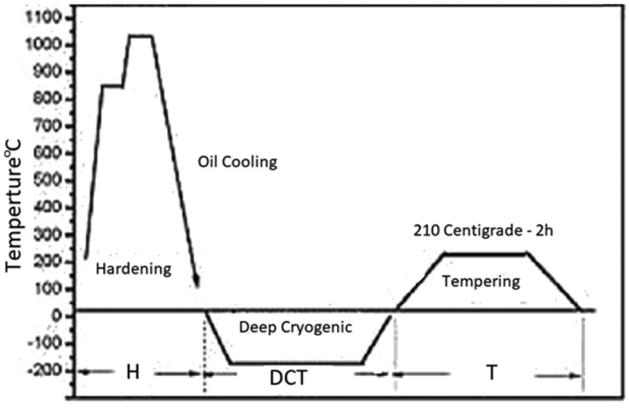

Figure 1: Application of cryogenic process.

cryogenic processes are composed of three stages including slow cooling, wetting, and tempering/heating [9].

Cooling step is the stage of cooling materials from ambient temperature to cold/cryogenic temperatures in a certain time interval (degrees/hours or degree/minutes). Wetting/Impregnation is the stage of keeping materials in cool/cryogenic temperatures within the specified time (hours), and this stage is important in terms of the resulting properties of the treated material. Tempering process is generally applied to metals to increase the fracture toughness of materials after the cryogenic process.

However, it is not recommended to conduct any tempering process before the cryogenic process in order to achieve the final effect [10]. It is stated in the literature that the cryogenic process increases many mechanical properties of iron alloys and non-iron alloys and wear lives exceeding 200% have been determined [11–13].

These days, energy saving has become a significant matter to take into account in the production of both consumer products and industrial equipment. Studies on energy saving, especially recent ones, have highlighted the required energy consumed in the sector [14–16] for the production of semi- and fully finished products. The industrial machining process is a primary component of the global economy. Identifying the optimal criteria for this process can contribute to the production of a maximum number of quality parts with minimum energy consumption [17,18]. Being a significant factor to evaluate mechanical components, roughness can also have an effect on their performance. Production costs and machining difficulties make having a low roughness value – which is desirable for such a process – difficult to achieve. These costs usually increase upon reduced surface roughness [19]. Numerous previous studies have focused on energy consumption in the machining process. Mori et al. [20] analysed the impact of cutting conditions on power consumption in the drilling and end milling of S45C carbon steel using a vertical machining centre. Liu et al. [21] milled ASSAB 760 steel under dry-cutting conditions and then measured the forces using a dynamometer and the power consumption using a Power Meter. Thus, a new machining energy consumption model was introduced. Camposeco-Negrete [22] determined optimal cutting parameters for minimal surface roughness, cutting force, cutting energy, and energy consumption for the turning of AISI 6061 T6. Oda et al. [23] conducted an experimental study to identify the optimal inclined angle for lowering the consumption of energy. In the turning of AISI 1045 steel, Shokoohi et al. [24] investigated the effect of the heat generated in the cutting zone on power consumption and workpiece quality.

Neugebauer et al. [25] analysed the effects of tool features on power consumption during the processes of drilling and turning. In addition, Muñoz-Escalona et al. [26] performed measurements of the energy consumption and surface roughness in the end milling of austenitic stainless steel under cryogenic, fluid coolant, and dry cutting conditions. Nas and Öztürk [27] performed face milling on a spheroidal graphite cast iron workpiece, measured the increase in the consumed power index (PI) using an ammeter device, and optimised the machining process through two different cutting tools. A model was prepared to determine the energy consumption allowance based on the movement of the workpiece within the machining system [28]. Surface roughness in the slot milling of Al-7075 was predicted through a proposed model. The hybrid technique used to develop the model was comprised of combined use of the analytically calculated SCEC (specific cutting energy consumption) and the experimentally characterized correlation between the SCEC and the surface roughness [29].

Unlike the studies in the literature, the threading process with the guide used widely in the industry was investigated in this study. In the industry, the pipe threading process is performed on machine tools specially developed for this job. These machines operate with the pitch system and perform the threading process by producing a high amount of torque for low shaft rotation speed. In this study, special energy consumption results, which have been widely considered an important output in machining processes in recent years, have been taken into account. In this context, the hardness, microstructure, and wear changes of the tap tools produced by powder metallurgy and casting method were examined in comparison with the energy consumption results. No study was found about the correlation between the microstructure and hardness changes of cutting tools and SEC (special energy consumption) results. In addition, the correlation between guide wear and microstructure and SEC has not been found in the literature. Unlike all the literature, the ideal tap tools material and heat treatment properties were investigated in this research in the light of the changes in these parameters. It is thought that this article can be a reference source for many studies.

2 Materials and method

This study was conducted by considering the maximum cutting torque and the mass production conditions in the industry. For this purpose, the pipe threading process was conducted in a single operation by using ¾" BSP (British Pipe Threading) female guide. A ¾" elbow which has a thin wall is among the materials having the highest cooling rate and which was designed in TS 11 EN 10242 standards was selected as the workpiece. The models were moulded in mechanical presses in a sand casting grade system on the pipe connection elements, and the casting was produced from GGG 42 material. Böhler 1.3343 High-Speed Tool steel bars produced by powder metallurgy method were supplied from the industry and threaded in the same way. Table 1 shows the chemical analysis of both types of materials.

High-speed tool steels heated in three stages to 1,250°C were quickly cooled with nitrogen. By applying the tempering process three times, the facture toughness was then increased. These processes were carried out in a vacuum environment, and then, the cryogenic process was applied to three different samples for 16 and 24 h at −80°C (Table 2). The samples were subjected to sanding and polishing by taking bakelite. Then, the etching process was done with 2% Nital. Microstructure images were obtained with an optical microscope. In addition, the microhardness changes were also investigated after heat treatment.

Table 3 shows the experimental plan designed for the threading process, and the process was performed with a product having three different heat treatment properties and at 30, 40, and 50 Hz frequency values. Thus, the effect

Table 2: Cutting tool production methods

Cutting tools	Production methods	Heat treatment
T1	Casting	Quenched
T2	Casting	Cryogenic (16 h)
T3	Casting	Cryogenic (24 h)
T4	Powder metallurgy	Quenched
T5	Powder metallurgy	Cryogenic (16 h)
T6	Powder metallurgy	Cryogenic (24 h)

Table 1: Chemical compositions of threading tools (mole%)

Material	Fe	C	Si	Mn	Cr	Mo	Ni	V	W
Powder metallurgy	80	0.717	0.399	0.286	4.15	5.04	0.323	1.89	6.59
Casting	77.9	0.81	0.617	0.637	4.87	5.41	0.68	2.15	6.12

Table 3: Experimental design for threading

Experiments	Cutting tools	Processes	Frequency (Hertz)
1	T3–T6	Cryogenic (24 h)	30
2	T3–T6	Cryogenic (24 h)	40
3	T3–T6	Cryogenic (24 h)	50
4	T2–T5	Cryogenic (16 h)	30
5	T2–T5	Cryogenic (16 h)	40
6	T2–T5	Cryogenic (16 h)	50
7	T1–T4	Quenched	30
8	T1–T4	Quenched	40
9	T1–T4	Quenched	50

of different heat treatment features applied to cutting tools on SEC results at different rotation speeds could be examined. For the first time in the literature, the effect of microstructure and hardness changes of a cutting tool on energy consumption and tool wear was discussed in this study.

In this manual threading machine, a current transformer and an ammeter were used during the pipe threading process in order to measure power indices (PI) (Figure 2). Thus, the graph in Figure 3 shows the power index changes. This graph shows that power index and power changes happened in three different regions.

During the turning process, the ecological effects of new cutting fluids were analysed using different cooling techniques, and energy consumption was measured. During the machining process, the power index (PI) measurement of the spindle servo drive was converted to kWh in this study via an ammeter through three-phase motor power conversion, as shown in equation (1).

$$P_{\text{Total}} = \sqrt{3}.\ V.\ I.\ \text{Cos}\sigma. \tag{1}$$

In this three-phase power conversion equation, P can be related to the power type and the torque of the motor. V stands for voltage, and it is 380 volts as it is an asynchronous motor. I is the current value, and the current index is measured with the help of an ammeter. The measurement of power index values in the first region is performed during the first time period. After the operator presses the start button, the guide starts to approach the workpiece. This time period can be called "approach time," and in this region, the guide advances with the engine speed determined by the inverter (P_{AAT}). In the second time period, the threading process takes place when the machine is idle ($P_{\text{Threading}}$) and the current used to carry out the threading process (P_{ATT}) is measured together with it (P_{Total}). The final period includes the separation of the product through the effect of friction under the return speed when the threading process is completed. The current changes are then measured during the progression to the switch and stopping of the motor (P_{ATT}). This period can also be classified as "retract time." During this period, a frequency of 100 Hz is provided using the inverter to save time and the guide moves to return with the maximum speed.

Specific energy consumption (SEC) represents the energy expenditure required to remove 1 ml of stock. It is associated with cutting mechanics. In addition, special cutting energy consumption (SCEC) is an important parameter for complete machinability. The energy consumption

Figure 2: Current index measurement with ampermeter (left), Bench where experiments are carried out (right).

value required to remove 1 ml of sawdust. When the machine does not remove chips in an empty state, it gives out except the energy it consumes. In other words, it can also be explained as the amount of energy spent just to remove the chip from the workpiece. Below are the equations [30] used in the calculations of these energy consumption results as equations (2) and (5):

$$P_{\text{Total}} = \sum_{j=1}^{Q_{ATT}} P_{\text{ATT}j}, \tag{2}$$

$$P_{\text{Threading}} = \sum_{j=1}^{Q_{\text{ATT}}} P_{\text{ATT}j} - \sum_{i=1}^{Q_{\text{AAT}}} P_{\text{AAT}i}, \tag{3}$$

$$\text{SEC} = \frac{\sum_{j=1}^{Q_{\text{ATT}}} P_{\text{ATT}j}}{\text{MRR}}, \tag{4}$$

$$\text{SCEC} = \frac{\sum_{j=1}^{Q_{\text{ATT}}} P_{\text{ATT}j} - \sum_{i=1}^{Q_{\text{AAT}}} P_{\text{AAT}i}}{\text{MRR}}. \tag{5}$$

3 Results and discussion

3.1 Microstructural evaluations

Figure 4 shows microstructure images of the guides produced with a typical casting method. As can be seen, cementite and partial martensite structures were encountered in the grain boundaries in the matrix structure made of pearlite islets, and no significant change was observed in the microstructure with the applied cryogenic process. This causes constant hardness values. Figure 5 shows microstructure images of the samples produced with the powder metallurgy method. As can be seen, precipitate phases shrunk relatively, their proportions increased visually, and they became more uniform. It was concluded that these precipitate phases in hard and brittle form were broken down and shifted in the structure due to the increased internal stresses during the cryogenic process. Similar observations are also available in the literature, carbide grains in the samples subjected to the cryogenic process were more evenly dispersed, and carbide volume in the microstructure doubled [31–34].

When Figure 6 was examined, typical cast dendritic branches formed grain boundaries, and MC carbides scattered into the coarse cast grains were seen. As seen in SEM images, microstructures of very different types were not encountered which made the hardness values constant. When Figure 7 was examined, MC carbides that were heavily precipitated are seen to be homogeneously dispersed. The tempering process led to the formation of different types of primary carbides. After the cryogenic process, the amount of carbides in the structure increased partially and the hardness increased as a result of a more homogeneous distribution of these carbides into the matrix. When Figure 7 was examined, Mo_2C–M_2C and Cr_7C_3–M_7C_3-type secondary carbides were observed to become more evident.

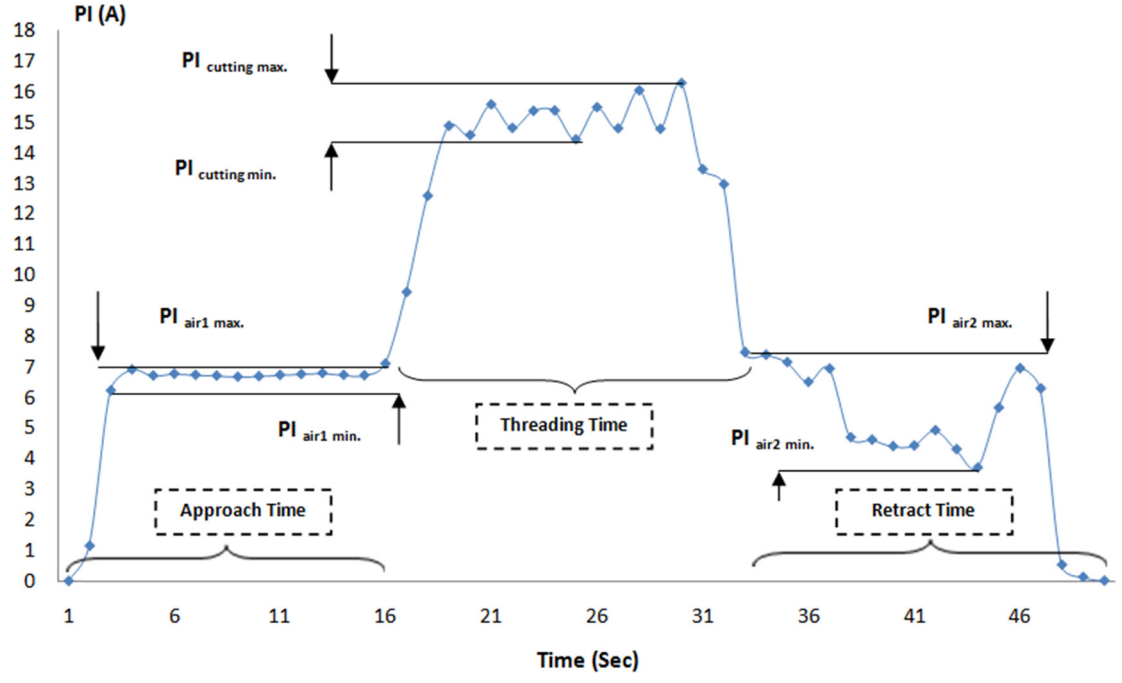

Figure 3: Power index changes.

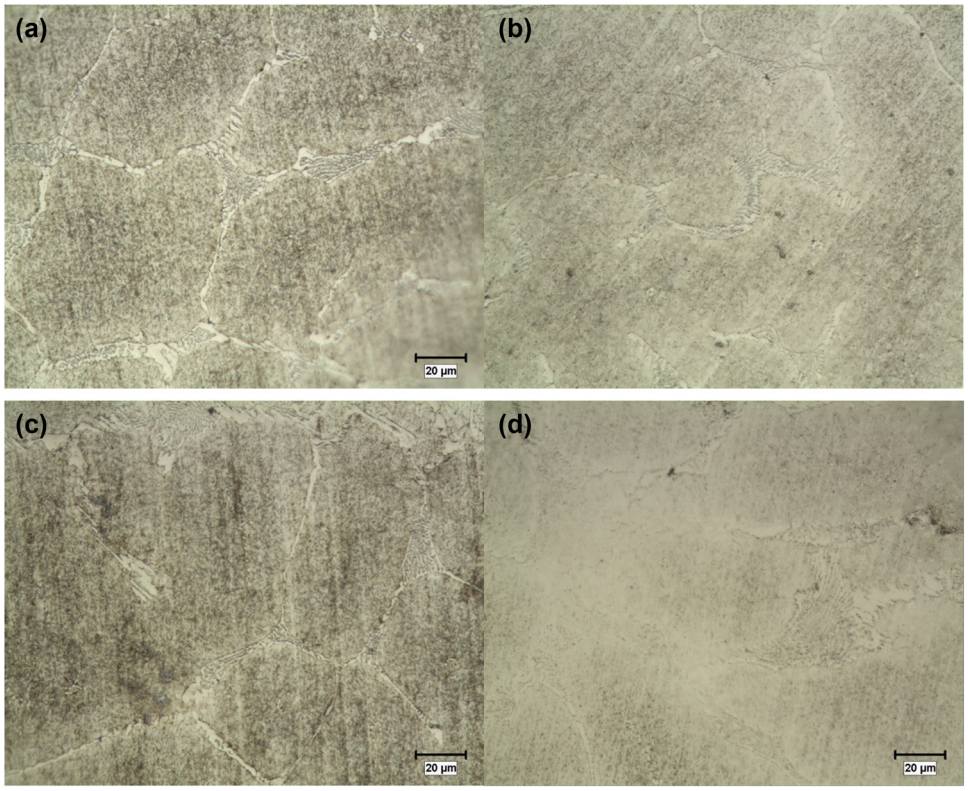

Figure 4: Optical microscope images of samples produced by casting: (a) untreated, (b) T1, (c) T2, and (d) T3.

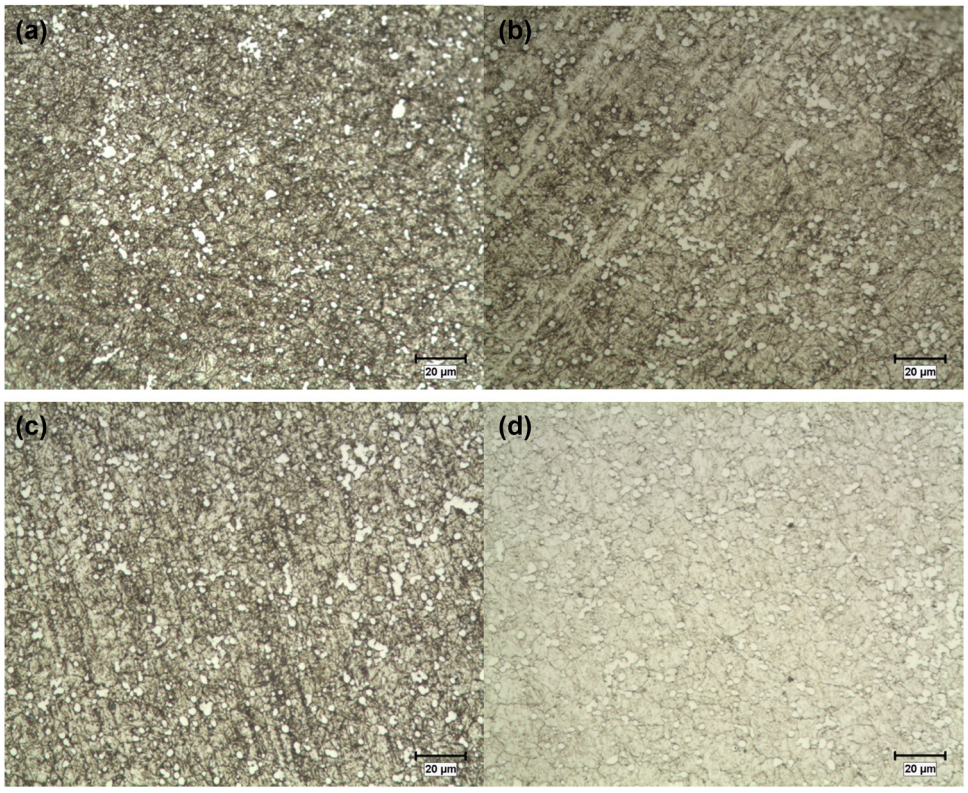

Figure 5: Optical microscope images of samples produced by powder metallurgy: (a) untreated, (b) T1, (c) T2, and (d) T3.

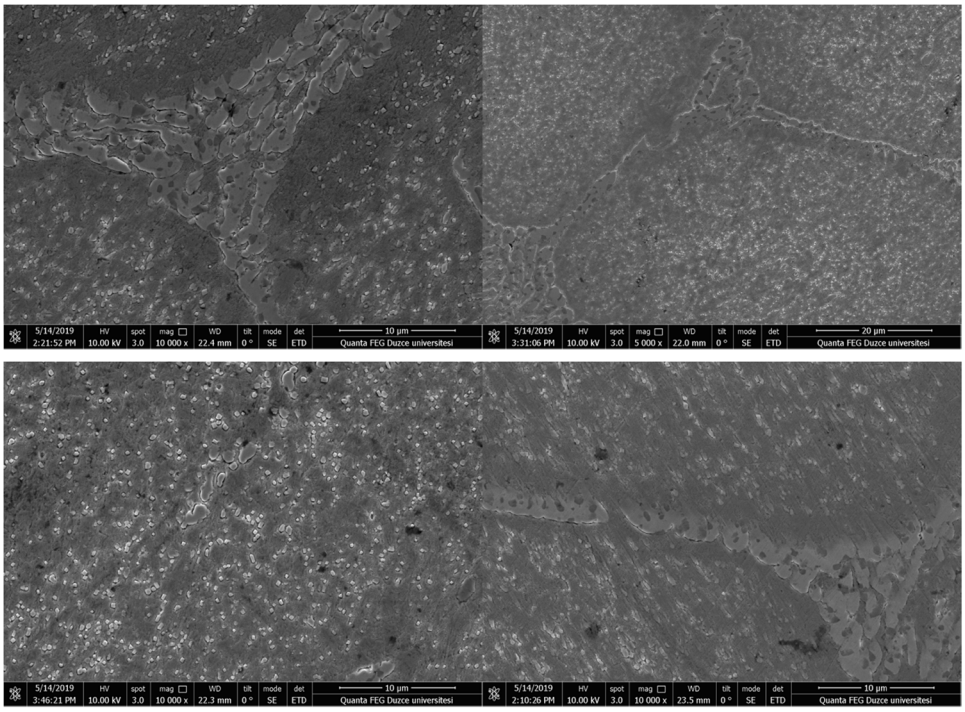

Figure 6: SEM images of the samples produced with casting.

When Figure 7 was examined, it can be seen that the grain boundaries emerged more clearly than the microstructure in Figure 6. In Figure 7, the basic structure consists of martensitic and a small amount of residual austenite. The 16-hour cryogenic process did not cause any significant change in the microstructure. When Figure 7 was examined, it was seen that Mo_2C–M_2C and Cr_7C_3–M_7C_3-type secondary carbides were denser and partially homogeneously distributed. With the cryogenic process, the residual austenite amount decreased more than the previous microstructure, and more MC carbide was formed, and they were observed to be distributed homogeneously in the matrix microstructure which increased the hardness values. Similar results were also obtained by ref. [13]. In the microstructure of the punches made from AISI D3 tool steels subjected to 24-hour and 36-hour deep cryogenic process at –145°C, the residual austenite amount decreased and MC carbides were homogeneously distributed. This resulting structure increased the punch life by causing an increase of hardness values. In addition, increasing cryogenic process time caused increases in both hardness and punch life. However, in a different study by the same researchers, deteriorations in corrosion properties were seen in contrast to these improvements [12,35].

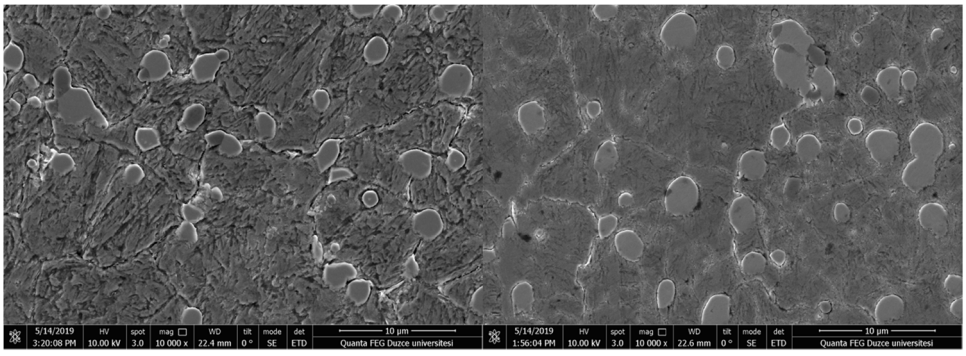

Figure 7: SEM images of the samples produced by powder metallurgy.

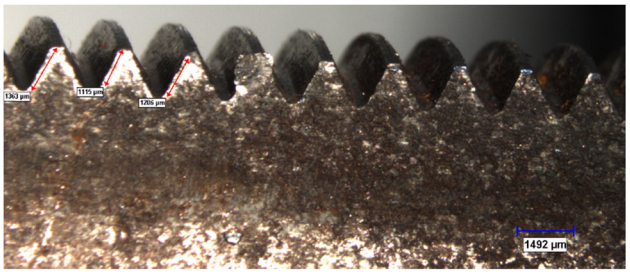

(a)

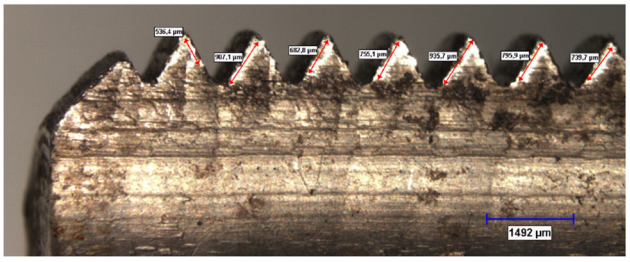

(b)

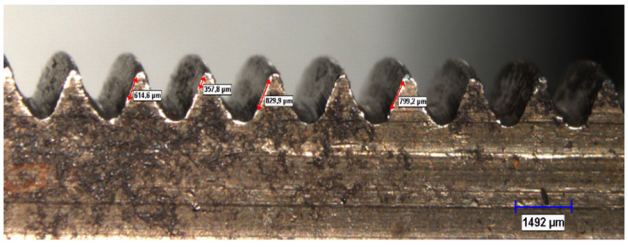

(c)

Figure 8: (a, b, c) Wear images of the samples produced by using the casting method.

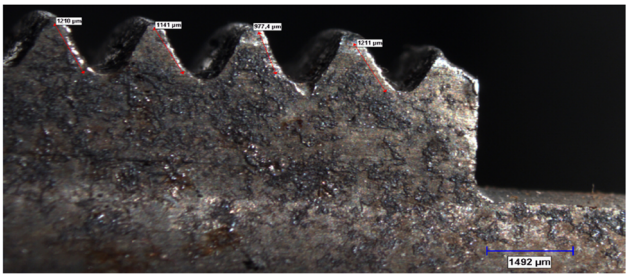

(a)

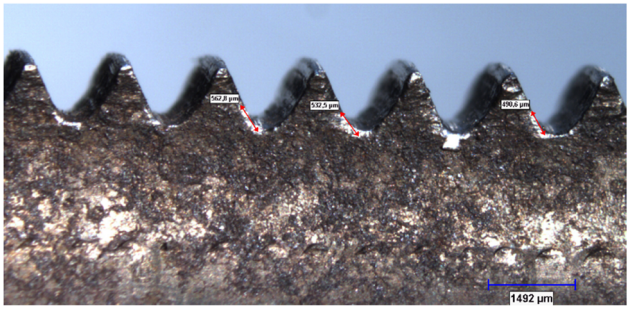

(b)

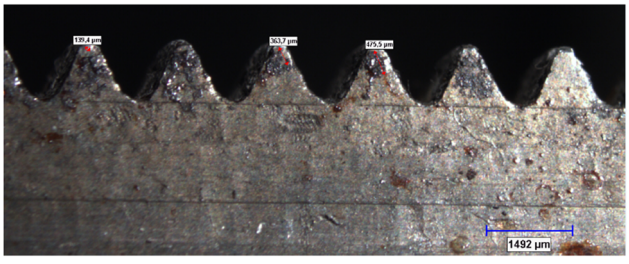

(c)

Figure 9: (a, b, c) Wear images of the samples produced by powder metallurgy.

3.2 Wear rate results

Wear rate obtained in each cutting process was measured with a light microscope. CLEMEX program equipped with a light microscope was used to determine the numerical value of the wear rate. The ISO standards for thread milling did not allow the wear rate to exceed VB = 0.8 mm. Therefore, the wear rate in the largest cutting length characterized by the bad scenario (the smallest tool life) was employed to determine the best optimum cutting conditions. Also, it can be observed that some materials adhere on the cutting edge (adhesive wear) during thread milling tests. Furthermore, some partial fractures and micro-cracks are caused by the forces on the cutting edge. These failures signify that the cutting tool has been significantly forced during the thread milling process of cast iron material (GGG 42). Figures 8 and 9 show optical images of each sample, and wear measurements were performed.

Table 4 shows the wear amounts obtained as a result of machining guide cutter tools produced with cast and

Table 4: Wear rates of thread tools

Production methods	Heat treatment	(Wear rate) V_B (µm)			VB_{ort} (µm)
Casting	Quenched	1,163	1,115	1,106	1,128
Casting	Cryogenic (16 h)	937.1	935.7	995.9	956.2
Casting	Cryogenic (24 h)	944.6	929.9	959.2	944.6
Powder metallurgy	Quenched	1,110	1,141	1,001	1,084
Powder metallurgy	Cryogenic (16 h)	562.8	532.5	490.6	529
Powder metallurgy	Cryogenic (24 h)	139.4	363.7	475.5	326

powder metallurgy methods with different cutting parameters of GGG-42 cast iron material in this study. When the results in Table 4 were examined, it can be clearly seen that the cryogenic process has an important effect on the wear amount. While this amount is very low in cast iron material, it can be asserted that cutting tools produced especially with powder metallurgy exhibited a much higher wear resistance performance than those produced with casting. This increase changed in parallel with the microstructure and hardness values. Compared to those treated with the cryogenic process, especially the wear resistance of the guide samples produced with powder metallurgy increased about four times. On the other hand, the wear amounts of both cast and powder metallurgical tools were very close to each other in the heat-treated samples.

3.3 Hardness results

Table 5 shows the mean hardness values of the guide tools subjected and not subjected to the cryogenic process and manufactured with the casting and powder metallurgy methods. While the mean hardness value of 741 HV was obtained in the guide tools not subjected to the cryogenic process and produced by the casting method, no significant hardness value change was observed in the samples for which the cryogenic process was applied. This process caused no effect on the microstructure of the samples produced by the casting method which did not reveal any change in the wear values and hardness values. However, while the mean hardness value was 844 HV in the untreated guides produced with powder metallurgy, significant increases were observed in the hardness values along with the increasing cryogenic process time, and these values reached 884 HV with the increasing time. The structure formed as a result of the hardening process was composed of martensite, residual austenite, and precipitate phases. It was thought that the amount of residual austenite in the matrix decreased with the

Table 5: Hardness results according to heat treatment conditions

Production method	Heat treatment type	Hardness (HV1)
Casting	Quenched	741
Casting	Cryogenic (16 h)	744
Casting	Cryogenic (24 h)	747
Powder metallurgy	Quenched	844
Powder metallurgy	Cryogenic (16 h)	871
Powder metallurgy	Cryogenic (24 h)	884

Table 6: Energy consumption results

Exper.	Material	Frequency	PI_{air} (A)	PI_{total} (A)	$PI_{cutting}$ (A)	P_{total} (kWh)	$P_{cutting}$ (kWh)	Time (s)	MR_{rate} (mmL)	SEC (Jul)	SCEC (Jul)
1	Cryogenic (24 h)	30	2.29	16.30	14.00	9.11	7.82	16.49	112.55	144.788	69.52
2	Cryogenic (24 h)	40	2.48	14.21	11.73	7.94	6.55	12.36	150.16	94.598	43.63
3	Cryogenic (24 h)	50	2.73	12.78	10.05	7.14	5.62	9.89	187.66	68.090	29.93
4	Cryogenic (16 h)	30	2.29	13.76	11.47	7.69	6.41	16.49	112.55	122.271	56.95
5	Cryogenic (16 h)	40	2.48	12.31	9.83	6.88	5.49	12.36	150.16	81.998	36.59
6	Cryogenic (16 h)	50	2.73	12.05	9.32	6.73	5.21	9.89	187.66	64.199	27.74
7	Quenched	30	2.29	11.99	9.70	6.70	5.42	16.49	112.55	106.505	48.15
8	Quenched	40	2.48	11.85	9.38	6.62	5.24	12.36	150.16	78.915	34.89
9	Quenched	50	2.73	11.51	8.78	6.43	4.91	9.89	187.66	61.356	26.16

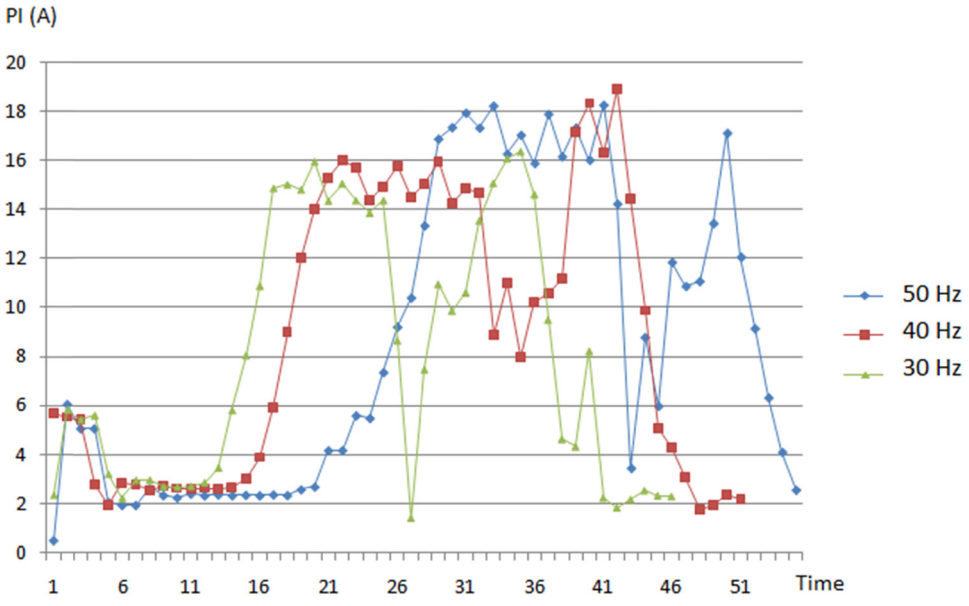

Figure 10: Energy consumption results (24 h).

cryogenic process, and the precipitate carbide phases were distributed more uniformly in the matrix phase, and this increased the hardness values.

3.4 Energy consumption results

The current changes according to the determined experimental design were measured while threading on the manual pipe threading machine. By using energy power conversion equations (1)–(5), power consumptions were calculated for all determined outputs (Table 6). The total current value was generally high at low-frequency values. This value decreased as the frequency increased. PI_{air} value providing information about the power consumption of the machine working in idle condition decreased in direct proportion with the frequency value. According to these results, it was believed that a more amount of instantaneous energy consumption was shown since the machine performed the

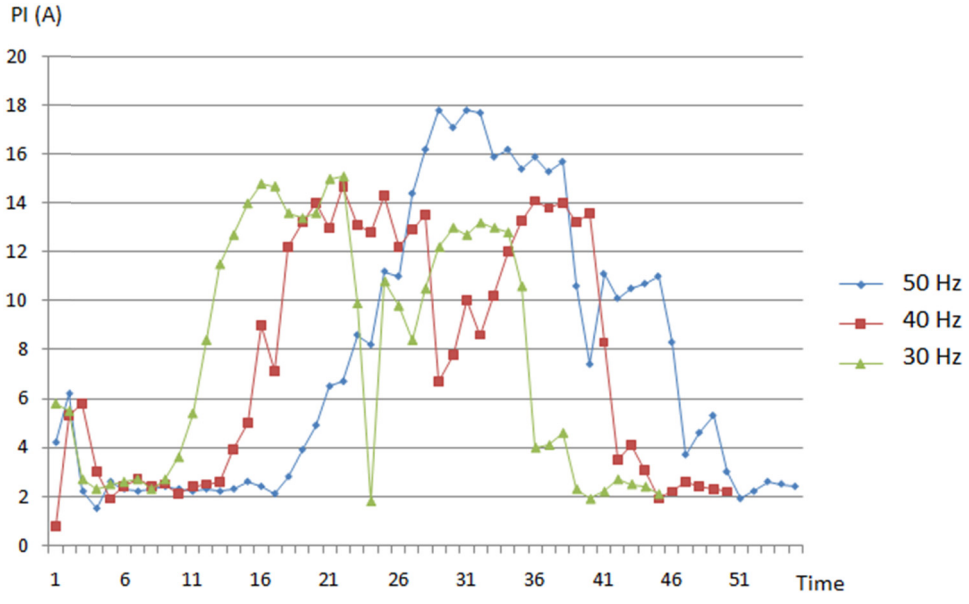

Figure 11: Energy consumption results (16 h).

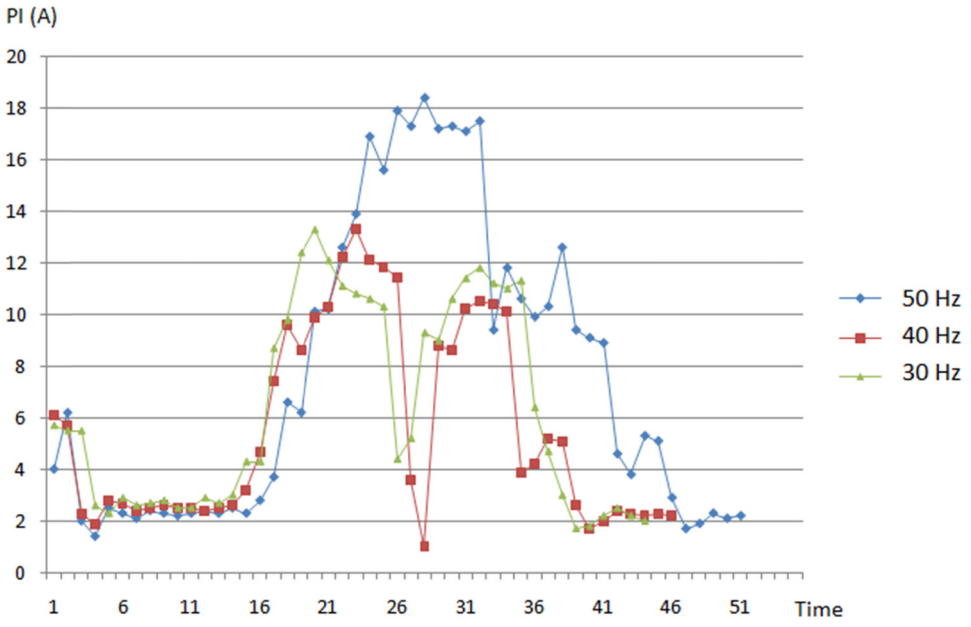

Figure 12: Energy consumption results, without heat treatment (24 h).

chip removal process with a lower rotation speed and a frequency lower than the ideal frequency value during the threading process although it performs less energy consumption while operating in idle position as the frequency value decreased [33,34]. When the instantaneous power consumption values (PI_{total}) were examined, power requirements showed variation between 9.11 and 6.43 kW. According to these results, it was determined that an average of 30% of energy can be saved by choosing the ideal cutting tools. SCEC results provided information about the machinability of a material, that is, the energy amount required to remove 1 mm^3 chips [20,31].

When SCEC results were examined, it can be asserted that the cold process applied to the cutting tool increased this value. The most possible reason for this was that the cutting tool increased the current value during residual threading of the cutting tool whose elasticity capability was lost and hardness value increased. When experiment 1 and experiment 4 were compared, the increase in SCEC value is proof of this theory. In addition, the SEC value was the most important output determining the energy consumption in mass production, and this value determined the energy consumption costs in production [21,25,28,36,37]. This value can be reduced from 144.788 J to 61.356 J by determining ideal cutting conditions. However, these ideal cutting conditions should be determined by examining the wear amount in cutting tools. Because cutting tool costs are an important factor that determines the production cost as much as the energy consumption. When the results were taken into consideration, the wear amount is less in the cutting tool produced with the powder metallurgy method. The least wear was achieved in a 16-hour cold treatment. In a threading process to be performed at a frequency of 50 Hz, the most appropriate energy spending will be 64.20 J. The time-dependent variation of the current changes obtained in the planned experimental setup is given in Figures 10–12. All calculations using the power-energy conversion equations were obtained and evaluated for these test results.

4 Conclusions

The guide tools produced with two different manufacturing methods (casting and powder metallurgy) were subjected to −80°C shallow cryogenic process, the effects of cryogenic process time, and manufacturing method on microstructure, and some mechanical properties were examined, and the following results were reached.

1. No significant microstructure and hardness changes were found in the guides produced by the casting method.
2. Significant changes were observed in both microstructural and hardness values in the samples produced with the powder metallurgy method. It can be said that increased cryogenic process time provided more uniform carbide distribution and a high martensite ratio affected hardness values.
3. By calculating the effect of manufacturing methods on wear mechanisms and lives of the guides and the

efficiency calculation, more qualified studies can be conducted.

4. While the shallow cryogenic process had little effect on the wear resistance in the guides obtained with the casting method, it provided up to four times improvements in the samples produced by the powder metallurgy method.
5. Cryogenic processes also affected energy consumption. While energy saving was not observed in the casting process, the value increases similar to wear resistance was also observed in energy savings.
6. When instantaneous power consumption values (PI_{total}) were examined, it was determined that an average of 30% energy savings can be provided by selecting ideal cutting tools. Accordingly, it was stated that the annual estimated energy saving will be approximately 6,174 kWh for this system by choosing the optimum operation conditions.

Funding information: The authors state stated no funding is involved.

Author contributions: All authors equally contributed to the preparation of the article.

Conflict of interest: The authors declare no conflict of interest.

Ethical approval: The conducted research is not related to either human or animal use.

Data availability statement: The data sets generated during and/or analysed during the current study are available from the corresponding author on reasonable request.

References

[1] Duman Ü, Dağlılar S. Katı Hal Kaynağı ile Birleştirilen AISI 3343 S 600-AISI4140 Çeliklerinin Araştırılması. Yıldız Teknik Üniversitesi Metalurji Dergisi. 2005;139:1–5.
[2] Rollason E, C. Metalurgy for engineers. London, UK: Edward Arnold; 1987.
[3] Okamoto H, Schlesinger M, Mueller E, (Eds.). ASM Handbook Volume 3: Alloy phase diagrams. Ohio, USA: ASM International; 2016.
[4] Drozda TJ, Wick C, Veilleux RF. Tool and manufacturing engineers handbook: Quality control and assembly. Dearborn, MI: Society of Manufacturing Engineers; 1983.
[5] TMMOB, TMMOB Metalurji Mühendisleri Odası Metalurji Dergisi, vol. 30, 1983.
[6] Steiner R. ASM Handbook, Volume 1: Properties and selection: Irons, steels, and high-performance alloys. Ohio, USA: ASM International; 1990.
[7] Bargel HJ, Schulze G. Malzeme Bilgisi. In: Güleç Ş, Aran A, (Trans.). İTÜ Ofset. İstanbul, Türkiye: 1987.
[8] Molinari A, Pellizzari M, Gialanella S, Straffelini G, Stiasny KH. Effect of deep cryogenic treatment on the mechanical properties of tool steel. J Mater Process Technol. 2001;118:350–5.
[9] Yamanoğlu O, Gül F. DIN 1.2379 ve DIN 1.2080 Soğuk İş Takım Çeliklerinin Sertlik ve Mikroyapısı Üzerine Kriyojenik İşlemin Etkisi, 2. Uluslararası Demir Çelik Sempozyumu (IISS'15). 1-3 Nisan, Karabük, Türkiye; 2007.
[10] Carlson EA. Cold treating and cryogenic treatment of steel in ASM Handbook, vol. 4 Heat Treating. 10th Ed. Metals Park, OH: ASM International; 1990. p. 203–6.
[11] Çiçek A, Ekici E, Uygur İ, Akıncıoğlu S, Kıvak T. AISI D2 Soğuk İş Takım Çeliğinin Delinmesinde Derin Kriyojenik İşlemin Takım Ömrü Üzerindeki Etkilerinin Araştırılması. Uluslararası Teknolojik Bilimler Dergisi. 2012;4(1):1–9.
[12] Akincioğlu S, Gökkaya H, Uygur İ. A review of cryogenic treatment on cutting tools. Int J Adv Manuf Technol. 2015;78(9–12):1609–27.
[13] Arslan Y, Uygur I, Jazdzewska A. The effect of cryogenic treatment on microstructure and mechanical response of AISI D3 tool steel punches. J Manuf Sci Eng. 2016;137(3):1–6. doi: 10.1115/1.4029567.
[14] Quan H, Chai Y, Li R, Peng G, Guo Y. Influence of circulating-flow's geometric characters on energy transition of a vortex pump. Eng Computations. 2019;36(9):3122–37.
[15] Liu S, Ding X, Tong Z. Energy absorption properties of thin-walled square tube with lateral piecewise variable thickness under axial crashing. Eng Computations. 2019;36(8):2589–609. doi: 10.1108/EC-10-2018-0492.
[16] Öztürk B. Energy consumption model for the pipe threading process using 10 wt.-% Cu and 316L stainless steel powder-reinforced aluminum 6061 fittings. Mater Test. 2019;61(8):797–805.
[17] Demir H, Gündüz S. The effects of aging on machinability of 6061 aluminium alloy. Mater Des. 2009;30:1480–3.
[18] Nas E, Gökkaya H. Experimental and statistical study on machinability of the composite materials with metal matrix Al/B4C/Graphite. Metall Mater Trans A. 2017;48(10):5059–67.
[19] Sukumar MS, Venkata Ramaiah P, Nagarjuna A. Optimization and prediction of parameters in face milling of Al-6061 using Taguchi and ANN approach. Procedia Eng. 2014;97:365–71.
[20] Mori M, Fujishima M, Inamasu Y, Oda Y. A study on energy efficiency improvement for machine tools. CIRP Ann. 2011;60:145–8.
[21] Liu N, Zhang YF, Lu WF. A hybrid approach to energy consumption modelling based on cutting power: A milling case. J Clean Prod. 2015;104:264–72.
[22] Camposeco-Negrete C. Optimization of cutting parameters for minimizing energy consumption in turning of AISI 6061 T6 using Taguchi methodology and ANOVA. J Clean Prod. 2013;53:195–203.
[23] Oda Y, Mori M, Ogawa K, Nishida S, Fujishima M, Kawamura T. Study of optimal cutting condition for energy efficiency improvement in ball end milling with tool-workpiece inclination. CIRP Ann. 2012;61:119–22.
[24] Shokoohi Y, Khosrojerdi E, Shiadhi BR. Machining and ecological effects of a new developed cutting fluid in combination

with different cooling techniques on turning operation. J Clean Prod. 2015;94:330–9.
[25] Neugebauer R, Schubert A, Reichmann B, Dix M. Influence exerted by tool properties on the energy efficiency during drilling and turning operations. CIRP J Manuf Sci Technol. 2011;4:161–9.
[26] Muñoz-Escalona P, Shokrani A, Newman ST. Influence of cutting environments on surface integrity and power consumption of austenitic stainless steel. Robot Computer-Integrated Manuf. 2015;36:60–9.
[27] Nas E, Öztürk B. Optimization of surface roughness via the Taguchi method and investigation of energy consumption when milling spheroidal graphite cast iron materials. Mater Test. 2018;60(5):519–25.
[28] Zhou X, Liu F, Cai W. An energy-consumption model for establishing energy-consumption allowance of a workpiece in a machining system. J Clean Prod. 2016;135:1580–90.
[29] Liu N, Wang SB, Zhang YF, Lu W. A novel approach to predicting surface roughness based on specific cutting energy consumption when slot milling Al-7075. Int J Mech Sci. 2016;118:13–20.
[30] Öztürk B. Investigation of effects of inverter frequency changes on the specific energy consumtion of pipe threading using response surface methodology. Measurement. 2020;152:107296.
[31] Babayan SA, Bairamov G, Abdulaliev Z. Optimization Of cutting conditions and tool geometry in multiple threading of tool joint threads. Chem Pet Eng. 1965;1(12):945–8.
[32] Arslan Y, Uygur I, Bayraktar H. Kriyojenik işlem uygulanmış soğuk iş takım çeliği zımba ile AISI 304 paslanmaz çelik saç malzemenin işlenebilme performansının araştırılması. İleri Tek Bilim Dergisi. 2013;2(83):61–75.
[33] Akyildiz H. Evaluating of cutting forces in thread machining. Int J Adv Manuf Tehnologies. 2013;1601–12.
[34] Khoshdarregi M, Altintas Y. Generalized modeling of chip geometry and cutting forces in multi-point thread turning. Int J Mach Tools Manuf. 2015;98:21–32.
[35] Uygur I, Gerengi H, Arslan Y, Kurtay M. The Effects of cryogenic treatment on the corrosion of AISI D3 steel. Mater Res. 2015;18(3):569–74.
[36] Zhao GY, Liu ZY, He Y, Cao HJ, Guo YB. Energy consumption in machining: Classification, prediction, and reduction strategy. Energy. 2017;133:142–57.
[37] Aktaş B, Toprak M, Çalık A, Tekgüler A. Effect of pack-boriding on the tribological behavior of Hardox 450 and HiTuf Steels. Rev Adv Mater Sci. 2020;59(1):314–21.